HHS Public Access

Author manuscript

Isr J Chem. Author manuscript; available in PMC 2017 January 11.

Published in final edited form as:

Isr J Chem. 2016 October ; 56(9-10): 705–723. doi:10.1002/ijch.201600022.

Redox Signaling through DNA

Elizabeth O'Brien, **Rebekah M.B. Silva**, and **Jacqueline K. Barton***

Division of Chemistry and Chemical Engineering, California Institute of Technology, Pasadena CA 91125

Abstract

Biological electron transfer reactions between metal cofactors are critical to many essential processes within the cell. Duplex DNA is, moreover, capable of mediating the transport of charge through its π-stacked nitrogenous bases. Increasingly, [4Fe4S] clusters, generally redox-active cofactors, have been found to be associated with enzymes involved in DNA processing. DNA-binding enzymes containing [4Fe4S] clusters can thus utilize DNA charge transport (DNA CT) for redox signaling to coordinate reactions over long molecular distances. In particular, DNA CT signaling may represent the first step in the search for DNA lesions by proteins containing [4Fe4S] clusters that are involved in DNA repair. Here we describe research carried out to examine the chemical characteristics and biological consequences of DNA CT. We are finding that DNA CT among metalloproteins represents powerful chemistry for redox signaling at long range within the cell.

Graphical Abstract

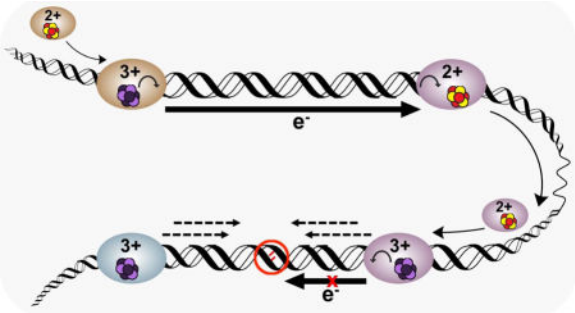

1. Introduction

Electron transfer reactions are integral components of fundamental processes in biology. These reactions often occur between two proteins that coordinate metals[1] such as Fe, Mn, Zn, or Cu. Metal centers in proteins can facilitate the single electron redox reactions central to biological processes such as respiration[2] and photosynthesis[3]. The mitochondrial respiratory chain, for example, involves several electron transfer processes, mediated by the metal cofactors in large, multiprotein complexes.[4–12] Several iron-sulfur centers and heme

*to whom correspondence should be addressed at jkbarton@caltech.edu.

proteins mediate redox activity essential to driving the oxidative phosphorylation that aerobic organisms use to generate energy.[2,4–6]

These redox reactions and others occur between donors and acceptors that are in relative proximity to one another; the electron transfer steps driving respiration occur within a single complex or between adjacent respiratory chain complexes in the mitochondrial membrane.[2,4–12] As established in beautiful studies by Gray and coworkers, biological electron transfer reactions can span over distances exceeding the single-step tunneling limit of ~20Å;[4] extensive studies with Ru- and Re-modified proteins[4,13–16] directly demonstrate intraprotein charge transfer over distances greater than this limit. Here, metalloproteins coordinate these reactions in multiple steps, using multistep electron tunneling, or electron hopping, through the insulating protein matrix. A strategically positioned aromatic residue such as tyrosine or tryptophan, with a relatively low ionization potential,[17,18] can increase the rate of electron transfer through a protein matrix.[14,16] A mutant azurin containing a covalent $[Re(CO)_3(dmp)]^+$ (dmp= 4,7-dimethyl-1,10-phenantroline) photooxidant coordinated by His 124 and a Trp residue engineered approximately halfway between the Cu (I) electron donor and photoexcited Re (II) acceptor, for example, has been demonstrated to transfer charge over a ~20Å distance approximately 100 times faster than the predicted time for the single-step tunneling reaction.[16] Nature can thus design proteins optimized for efficient redox chemistry within a macromolecule or a complex, but can biological electron donors and acceptors also couple with one another from still longer distances, to coordinate a genome-wide process such as DNA repair?

Here we focus on electron transfer reactions across DNA, another important biological macromolecule. We describe the extensive characterization of this chemistry in many laboratories and how study of long-range electron transfer through DNA led us also to examine the redox chemistry of DNA processing enzymes that coordinate iron cofactors. The ubiquity of [4Fe4S] clusters being associated with enzymes involved in DNA processing has led us to consider roles where electron transfer reactions through DNA might be beneficially applied. This review is not exhaustive, but it is intended to illustrate the unique features of DNA charge transport chemistry and how these features may be utilized within the cell.

2. Fundamentals of DNA Charge Transport

Electron transfer through protein matrices occurs on the microsecond timescale,[4] mediated by σ bonds and hydrogen bonds. Electron transfer reactions occur through duplex DNA, however, at a significantly faster rate.[19–27] DNA-mediated charge transport (DNA CT) is mediated by the π-stacking interactions of the nitrogenous bases at the center of the DNA helix and occurs on the picosecond timescale.[27] The aromatic bases, stacked in 3.4 Å layers, contain overlapping π orbitals in a structure closely resembling that of stacked graphene sheets (Figure 1). After observing this similarity in structure between DNA and graphite in the dry, solid state, Eley and Spivey[28] along with others predicted that the DNA helix, based upon its chemical structure, would conduct charge. Our laboratory has observed that DNA-mediated charge transport occurs over long range[22,26] and is shallowly dependent on molecular distance traveled.[23,26,29–31] DNA CT indeed occurs through the

nitrogenous base pairs, whose overlapping π orbitals provide a pathway for charge to travel down the helical base pair stack.[19–31] This property is additionally exquisitely sensitive to perturbations in the stacking interactions of the bases, such as those that occur with base-pair mismatches and lesions.[23,29–31]

Studies of DNA CT by our laboratory and others have prompted several proposals about the mechanism through which CT occurs under aqueous, biologically relevant conditions. [23,25–39] Superexchange between DNA bases was proposed but cannot explain the long molecular distances over which DNA-mediated CT is observed.[32–35,40] Localized hopping has also been suggested to mediate DNA CT, as charge can migrate along DNA through superexchange between neighboring guanine bases in the sequence.[41] This model, however, cannot fully explain the weak distance dependence of DNA CT consistently demonstrated[42–44] or the attenuation of DNA CT in the presence of base-pair mismatches.[23,26,29–31] Delocalization of charge likely occurs through transient interactions influenced by dynamic changes in the duplex DNA structure in solution[27,38,45] and perhaps also formation of polarons in the vicinity of charge moving through DNA.[36,37,39] Long-range, shallowly distance-dependent DNA CT thus depends on several factors and cannot be adequately explained by a single mechanism. Charge migration through DNA likely occurs through a variety of pathways, with some delocalization over DNA domains gated by the DNA conformational dynamics.[38,46]

Though these studies have demonstrated a variety of mechanistic processes at work during DNA CT, they also consistently demonstrate its key properties under all conditions assayed. DNA charge transport occurs over long molecular distances[29–31,38,46–48] and exhibits a shallow dependence on distance traveled.[29–31,40,46–49] Charge transfer through DNA furthermore requires coupling of electron donors and acceptors into the π-stack and is attenuated in the presence of perturbations in the base stacking interactions, such as base-pair mismatches,[23,29–31] bulky lesions in the duplex sequence,[50] or severe structural distortion of the helical stacking.[51,52] These fundamental characteristics all suggest that Nature may harness DNA CT during the search for and subsequent repair of DNA damage sites, which attenuate charge transport.

3. DNA-binding Proteins contain [4Fe4S] Clusters

Duplex DNA with well-stacked bases is thus a strikingly effective mediator of charge transport, but what proteins serve as the electron donors and acceptors? In order to utilize DNA CT for long-range redox reactions, electron donors and acceptors must both possess a metal center capable of one-electron transfer reactions and bind duplex DNA such that their redox centers are coupled into the π-stacked bases. Cunningham and coworkers initially discovered[53] in 1989 that the base excision repair (BER) glycosylase Endonuclease III (EndoIII) in *E. coli*, which repairs oxidized pyrimidine bases[54] in genomic DNA, contains a [4Fe4S] cluster cofactor. Several other DNA repair proteins including BER glycosylase MutY (*E. coli*),[55] family 4 Uracil-DNA glycosylase from thermophiles (UDG),[56] Nucleotide excision repair helicase XPD (*S. acidocaldarius*) (*Sa*XPD),[57] and R-loop maturation helicase DinG (*E. coli*)[58] have since been discovered to contain [4Fe4S] clusters. The transcription factor SoxR, which binds DNA and activates transcription of *soxS*

genes to defend the cell during oxidative stress, has additionally been shown to contain a [2Fe2S] cluster cofactor.[59] Remarkably eukaryotic DNA polymerases and DNA primase were also recently shown to contain[4Fe4S] centers.[60,61]

Iron-sulfur cofactors, such as the rhomboid [2Fe2S] cluster and cubane [4Fe4S] cluster (Figure 2), are often agents of redox chemistry in biology, with a tunable range of potentials from 300mV to below −500mV vs. NHE.[62] These species likely arose during prebiotic conditions on Earth, when an abundance of ferrous iron and sulfide would have been present in the atmosphere.[63] These cofactors are generally coordinated by conserved cysteine motifs, and require a large group of proteins to assemble and load the clusters into their recipient proteins.[1,64,65] Incorporation of an iron-sulfur cofactor into a protein is a complex and metabolically expensive task for cellular machinery, requiring biogenesis and assembly proteins, chaperone proteins for transport, and in the case of eukaryotes, a targeting complex comprising of three proteins (CIA1, CIA2, and MMS19)[64–66] to load the cofactor into its recipient protein.

The general process for iron-sulfur biogenesis and loading is summarized in Figure 2. In bacteria, the ISC assembly machinery is generally responsible for cofactor generation, though the NIF system has been identified as part of the maturation pathway for the iron-sulfur containing enzyme nitrogenase and the SUF assembly system is implicated in biogenesis during oxidative stress.[1] In eukaryotes, the ISC assembly machinery and mitochondrial ISC export system are necessary for biogenesis of the cofactor[67] and the cytosolic iron-sulfur assembly (CIA) machinery is required for cluster maturation.[68,69] Inorganic sulfur is acquired from a cysteine desulfurase (IscS) in bacteria or exported from the mitochondria by Atm1,[67,70] then bound by a cysteine desulfurase (NFS1) in eukaryotes. Cysteine desulfurase activity converts cysteine to alanine, generating a persulfide which is then transported directly or indirectly to scaffold proteins (IscU in bacteria, ISU in eukaryotes) for cluster assembly. Ferrous iron is donated by a protein source, and electron transfer occurs to reduce S^0 to S^{2-} present in iron-sulfur clusters. After the *de novo* biosynthesis of a labile cluster coordinated by scaffold protein cysteine residues, the cluster-containing scaffold associates with chaperone proteins (HscA/HscB in bacteria, HSC20/HSPA9 in eukaryotes). ATP hydrolysis likely drives a conformational change in order to keep the labile cluster shielded during delivery to the recipient protein,[1,64] and direct or indirect transfer of the cofactor to the recipient protein occurs.

Creation and incorporation of iron-sulfur clusters into proteins is thus a metabolically expensive task requiring the engagement of several protein systems. Placing an iron-containing cofactor in a DNA-binding protein could additionally place the bound nucleic acid at risk of damage. A labile ferrous iron from the cofactor could react with hydrogen peroxide in the cellular environment; this Fenton chemistry creates reactive oxygen species (Figure 2) which could damage nearby DNA bases. Why then does Nature spend the requisite energy incorporating a redox-active inorganic cofactor into a DNA-processing enzyme?

4. Platforms to Study DNA CT

The development of new methods was necessary to test whether DNA conducted charge in solution at ambient temperatures. Certainly, assessing potential biological roles for DNA CT chemistry requires experiments to be performed in aqueous solution using physiologically relevant conditions. Key properties of DNA charge transport have now been characterized extensively, through the development of several robust and versatile platforms.[19–27, 50–52–71–81] DNA CT has been studied in the excited state and the ground state, as well as using single- molecule assays. Across all of the platforms developed, consistent features of DNA CT are observed: (*i*) charge transport through duplex DNA is dependent on the coupling of redox donors and acceptors to the π-stacked bases; (*ii*) DNA CT can occur over long molecular distances with shallow distance dependence; and (*iii*) DNA CT is attenuated in the presence of even minor perturbations in π-stacking interactions between the bases.

Our laboratory initially assayed the charge transport properties of DNA using photophysical studies, employing DNA-intercalating redox donors and acceptors. We covalently appended metal complexes such as $[Ru(phen)_2dppz]^{2+}$ (phen= 1,10 phenanthroline, dppz = dipyrido[3,2-*a*:2′,3′-*c*]-phenazine) and $[Rh(phi)_2(phen)]^{3+}$ (phi = 9,10-phenanthrenequinone diamine) to a short, 15-bp oligonucleotide.[19] These metal complexes intercalate into the duplex DNA bases and upon irradiation, $[Ru(phen)_2dppz]^{2+}$ acts as a luminescence donor, which is quenched through an intra-duplex mechanism by the $[Rh(phi)_2(phen)]^{3+}$ acceptor. (Figure 3) When an oligonucleotide modified with the $[Ru(phen)_2dppz]^{2+}$ donor and $[Ru(phen)_2(phen')]^{2+}$ (phen′= 5-amido-glutaric-acid-1,10-phenanthroline), a poor DNA intercalator, is irradiated, luminescence is no longer quenched, suggesting a mechanism dependent on intercalation, which is required for coupling of the donor and acceptor into the DNA duplex.

To investigate further the mechanism of charge transport through DNA bases, we assayed luminescence quenching of fluorescent base analogues 2-aminopurine (A_2) and 1,N^6-ethenoadenine (A_ε) by guanine (G) or deazaguanine (Z)[25] which possess low enough redox potentials to act as acceptors.[82] This assembly allowed for investigation of DNA CT without potential constraining effects of covalent intercalating metal complex donors and acceptors on the DNA helix structure. A long-range, shallowly distance-dependent mechanism of quenching for A_2, which couples well into the DNA π stack, was observed. This mechanism was not observed, however, for the bulkier A_ε analogue, which is less capable of π-stacking and thus less effective in coupling into duplex DNA.[25] Fluorescence quenching of a DNA-intercalated ethidium donor by a $[Rh(phi)_2(bpy)]^{3+}$ acceptor through a 17-bp DNA duplex, moreover, is fivefold less efficient in the presence of a single CA base pair mismatch, relative to a well-matched duplex.[23] These results together suggest that well-stacked DNA bases are essential for charge transfer through DNA; perturbing the π-stacking interactions severely attenuates DNA CT.

Using DNA-intercalating photooxidants, we have also observed DNA charge transport or DNA damage generated at a distance. An intercalating oxidant such as $[Rh(phi)_2(bpy')]^{3+}$ (bpy′= 4-butyric acid, 4′-methylbipyridine) can be tethered to one end of a 63-bp duplex

DNA substrate and photoexcited, oxidizing low-potential guanine bases at the 5′-end of a 5′-GG′-3′ doublet sequence.[26] (Figure 3) Photolysis leads to the oxidation product 7,8-dihydro-8-oxo-2′-deoxyguanosine (8-oxo-G) to form in a DNA-mediated manner, observed up to 200 Å from the site of intercalation. These reactions also have been demonstrated to occur on the picosecond timescale;[27] charge can move 10 times the single-step tunneling distance through protein in a miniscule fraction of the time!

Additional platforms have been used to study DNA CT in the excited state, elucidating the mechanisms at play during a DNA-mediated charge transport event. Injection of charge through photoexcitation of a 4′-acylated nucleotide at the 3′-end of a duplex oligonucleotide oxidizes low-potential guanine bases at a distance and corroborates the shallow distance dependence observed in experiments measuring guanine damage.[40] Theoretical modeling, in conjunction with photooxidation of DNA hairpins bridged with a stilbene-derivative, [83–85] also demonstrate that DNA CT occurs at a distance and these results also could not be explained exclusively by a coherent superexchange mechanism.[33] Photoexcited anthraquinone, (Figure 3), tethered to one end of a duplex DNA substrate, can also be used to damage guanine bases in an oligonucleotide sequence.[36,38,39,46] Schuster and coworkers employed this platform, along with computational modeling of DNA interactions with Na^+ counterions and water molecules in solution, providing results consistent with environment-dependent partial charge delocalization on DNA.[39]

After observing rapid, long-distance, and mismatch-sensitive DNA CT in the excited state, methods to study DNA CT in the ground state were also developed. Our laboratory has utilized both a single-molecule[79,80] and a multiplexed electrode[76–78] platform to study ground-state DNA CT. In the single-molecule platform, a gap is first chemically etched into a single-walled carbon nanotube (SWCNT). A molecule of single-stranded DNA (ssDNA) modified with an amine group at both ends, is covalently attached through amide coupling to the oxidatively etched SWCNT, functionalized at the ends with a carboxylic acid group.[79] A well-matched complementary strand, or a strand containing a single-base mismatch, is then annealed to the ssDNA bridging the etched nanotube. This assembly creates a circuit (Figure 4) that allows for measuring the conductance of a single DNA molecule relative to the nanotube. The source-drain current measured using this platform demonstrates that charge flows through well-matched, but not mismatched, DNA duplexes. Site-specific restriction enzyme[79] and methyltransferase activity[80] have moreover been demonstrated on duplex DNA substrates in this setup; the DNA circuit is biologically accessible.

Additional single-molecule platforms to study ground-state DNA CT, based on readout from electrochemical atomic force microscopy (AFM) or scanning tunneling microscopy (STM),[47,48,71] have been designed and used to measure conductance through an oligonucleotide. Tao and coworkers[71] measured passage of current at different applied voltages through a single 8-bp dsDNA substrate. The DNA is modified at both ends with alkanethiol groups, with one end covalently attached to an Au surface and the other end free to link covalently to a gold STM tip brought into close contact with the DNA-modified gold surface. This study demonstrated consistently high conductance of duplex DNA and a shallow distance dependence for DNA CT, relative to electron transfer through σ-bonded species.

Electrochemical AFM studies of conductance through a single DNA molecule have also been performed by Porath and coworkers,[47,48] using the platform design in Figure 4. A single strand of DNA (26 nucleotide length) is attached to a gold surface through an alkanethiol moiety. This strand is hybridized to a complementary strand, which is covalently attached to a gold nanoparticle through an alkanethiol moiety. An electrochemical AFM tip can then contact the gold nanoparticle on the end of the duplex DNA substrate and measure conductance through the oligonucleotide. This platform demonstrated high conductance through 26 base pairs of DNA,[47] consistent with other single molecule studies.[71,79,80] It was additionally used to demonstrate that duplex DNA, but not single-stranded DNA, is able to conduct charge.[48]

The SWCNT circuit, STM, and electrochemical AFM platforms for studying ground-state DNA CT through a single molecule are complemented by studies using the multiplexed DNA-modified gold electrode platform.[76–78] (Figure 4) This high-throughput system facilitates obtaining reproducible electrochemical readouts for ground-state, aqueous DNA CT under different conditions (well-matched versus mismatched duplex DNA, for example), all on a single electrode surface. DNA-modified gold surfaces are first constructed by incubating a duplex DNA substrate with an alkanethiol moiety at one end on the Au(1,1,1) surface, allowing a covalent thiol-gold attachment to form. The DNA molecules then form a densely packed self-assembled monolayer on gold, oriented at a 45° angle relative to the electrode surface, as shown using AFM.[86] After the gold surfaces are incubated with alkanethiol-modified DNA and any remaining bare gold is passivated using β-mercaptohexanol,[76–78] the DNA-modified surfaces become the working electrode in a three-electrode cell setup, with a silver/silver chloride reference and a platinum auxiliary electrode. Electrochemical techniques such as cyclic voltammetry (CV), square wave voltammetry scanning, and bulk electrolysis can be used to monitor the DNA-mediated passing of charge between the gold surface and a redox-active species at the distal end of the DNA duplex, over a physiologically relevant range of potentials.[24,50,51,72–78,82,86–94]

The multiplexed electrode system (Figure 4) was adapted from a single-surface DNA-modified electrode platform developed in our laboratory[24,87] and allows for scanning of 16 DNA-modified electrodes on a single surface. The gold electrodes, each with an area of $2mm^2$, are arranged in four quadrants on the silicon chip.[76] These quadrants are divided physically from one another in the multiplex chip setup for electrochemistry, so that as many as four different DNA substrates can be incubated on one chip. In this manner, facile, reproducible readouts for a new experimental condition can be obtained alongside control experiments; there is no longer a need to measure two conditions for the same experiment on different gold surfaces.

Using our DNA-modified electrode platform, we have observed properties of DNA CT consistent with the results of photophysical and single-molecule studies, obtaining readouts from both redox-active dyes such as Nile Blue[51,77,94] and DNA-bound enzymes with redox-active [4Fe4S] clusters (*vide infra*).[72–75,78,88,89,92] DNA-mediated redox signals on the gold electrode are contingent upon coupling of the redox-active species to the π-stacked bases.[23,91] DNA CT additionally has been observed over long distances on this platform; a DNA-mediated signal for the redox probe Nile Blue was observed over 100 bp (34nm) of

DNA. The signal through 100 bp of duplex DNA remarkably displays the same kinetics and mismatch sensitivity as a redox signal through 17 bp of DNA. The distance dependence of DNA CT in the ground state is shallow; the rate-determining step is electron tunneling through the alkanethiol linker.[77] Finally, DNA CT has been shown to be sensitive to perturbations in the base-stacking interactions using this platform; DNA-mediated electrochemical signals are attenuated in the presence of base pair mismatches,[23,76,77,95] bulky lesions,[50] and structural distortions such as bending of the upright helix through binding of TATA-binding protein.[51,52]

The duplex DNA substrates on the multiplex electrode surfaces, importantly, are present in a biologically accessible conformation. We have demonstrated, for example, that when a binding site for restriction enzyme *RsaI* is engineered into the 100-bp DNA substrate on the multiplex chip platform, *RsaI* will bind the DNA and cut at the restriction site when incubated on the Au electrode.[77] We have additionally demonstrated methyltransferase activity on these electrodes, in a setup with a signal-on detection based on the readout from a Nile Blue signal.[94] These enzymatic activity readouts were based on redox probe signals, but we have also been able to monitor the DNA-bound electron transfer activity of enzymes with [4Fe4S] clusters using these electrodes. Incubation of [4Fe4S] repair helicases *Sa*XPD[92] and DinG[73] (*E. coli*) on DNA-modified gold electrodes produces a large, ATP-dependent DNA-mediated redox signal, associated with the coupling of the [4Fe4S] cofactor to the duplex DNA; interestingly, coupling increases with ATP-dependent helicase activity.

Many research groups have thus developed systems which have allowed for characterization of the electronic properties of DNA along with effective methods to test how DNA charge transport may be used in biology. This long-range, rapid chemistry is sensitive to perturbations in the base-stacking interactions, and these characteristics have consistently and reproducibly been seen in the ground state and the excited state, on single-molecule, ensemble, and multiplexed platforms. Building on the foundation of these robust *in vitro* methods, we can therefore investigate the DNA-mediated charge transfer properties of biological systems and how this chemistry is utilized within the cell.

5. DNA Charge Transport in Biology: Initial Observations

After characterizing the fundamental properties of DNA charge transport on a molecular level using chemical and physical methods, we next focused on answering the question: can DNA CT operate in a cellular environment, modulating reactions at a distance as it does *in vitro*? The first important question to answer was whether DNA CT occurred in cell nuclei,[96] where genomic DNA is produced and stored. Upon treatment of HeLa cell nuclei with the DNA-intercalating photooxidant $[Rh(phi)_2DMB]^{3+}$ (DMB = 4,4′-dimethyl-2,2′-bipyridine), we observed long-range oxidation of guanine bases at the 5′-positions in 5′-GG-3′ doublet and 5′-GGG-3′ triplet sequences upon irradiation of the samples to photoexcite the Rh(III) compound. Damage at 5′-guanines in 5′-GGG-3′ and 5′-GG-3′ sites, a signature of DNA-mediated one electron oxidation, was furthermore demonstrated in mitochondria, [97] upon irradiation of a Rh(III) intercalating photooxidant. Long-range oxidation of low-potential guanine sites occurred in cells, affecting regions to which proteins were known to bind and those free of proteins; [96] for example the binding of a transcription

factor[96] did not inhibit DNA-mediated damage of guanine residues; charge can migrate through bases as long as the helical structure and stacking interactions are not distorted.

We also investigated whether DNA CT could occur through duplex DNA bound in a nucleosome core particle (NCP), the fundamental unit of DNA packing in eukaryotic cells. (Figure 5) An octameric complex of histone proteins binds and wraps ~150 bp of duplex DNA in an NCP structure, which then is further assembled into higher-order structures in the nucleus. [98,99] Since a large portion of the eukaryotic genome is bound in these structures, which curves the helix gently around the histone core, it is relevant to ask whether CT can occur through histone-bound DNA to affect genome-wide reactions. Using the DNA-intercalating $[Rh(phi)_2(bpy)]^{3+}$ photooxidant tethered to DNA in the presence and absence of histones, we observed long-range oxidative damage to 5′-guanine bases in 5′-GG-3′ doublets and 5′-GGG-3′ triplets.[100] As DNA CT occurs in histone-bound, packaged DNA, it is a feasible mechanism for genome-wide signaling and sensing of oxidative stress conditions in eukaryotic cells. This result also confirms further that DNA CT can occur through protein-bound DNA as observed in HeLa cell nuclei, as long as the π-stacking base interactions are maintained.

Protein binding which does perturb the coupling of the π-stacked bases, however, can modulate charge transfer through DNA. TATA-binding protein (TBP), for example, is a ubiquitous transcription factor that bends DNA approximately 80° when it binds.[101] We have demonstrated using our DNA electrochemistry platform that TBP attenuates DNA CT in binding and severely kinking the double helix, disrupting base pair π-stacking interactions.[51] TBP binding and kinking of the DNA double helix therefore allows for modulation of redox reactions at a distance by changing the CT properties of protein-bound DNA. This modulation is reversible, occurring only when TBP is bound to a segment of duplex DNA. It is dependent on the structural properties of the DNA helix in the presence or absence of a binding event and suggests that proteins, in modulating DNA CT, can play a range of regulatory roles during the cell cycle.

One important dynamic condition in the cellular environment which requires a biological response is oxidative stress.[102] SoxR is a transcription factor in enteric bacteria containing a [2Fe2S] cluster and is responsible for binding the *soxS* promoter in the bacterial genome to activate transcription of genes to respond to oxidative stress in the cell.[102,103] SoxR binds DNA as a dimer, and the apo-form, which does not contain the cluster, binds with a similar affinity as the holoenzyme containing the [2Fe2S] cofactor.[104] The transcriptional activation activity, however, is dependent on the cluster.[105] We showed using DNA electrochemistry that SoxR undergoes a potential shift of +490mV when bound to DNA, suggesting that the DNA-bound protein is generally in the reduced $[2Fe2S]^+$ state but can be oxidized to the $[2Fe2S]^{2+}$ state at cellular potentials where oxidative stress arises.[52] SoxR is capable of DNA-mediated redox activity when bound to DNA, but can this transcription factor respond to oxidative stress at a distance in a DNA-mediated manner?

To investigate whether DNA charge transport can modulate the redox state, and therefore the transcriptional activity, of SoxR at a distance, we employed DNA-intercalating photooxidants. We demonstrated with noncovalently bound $[Ru(phen)(dppz)(bpy')]^{2+}$

(dppz = dipyridophenazine, bpy′= 4-butyric acid 4′-methyl bipyridine), that reduced $[2Fe2S]^{+}$ SoxR can become oxidized to fill guanine radicals created by the Ru(II) oxidant upon irradiation. We then examined directly whether this oxidation of SoxR could be mediated by DNA.[106] Using a DNA-intercalating $[Rh(phi)_2(bpy′)]^{3+}$ photooxidant tethered to one end of a 180-nt duplex DNA substrate, which contained the SoxR binding sequence in the *soxS* promoter 80-nt from the site of intercalation, we were able to observe not only oxidation and but also activation of bound, transcriptionally silent $[2Fe2S]^{+}$ SoxR through DNA. (Figure 5) The irradiated $[Rh(phi)_2(bpy′)]^{3+}$ promotes transcriptional activity associated with oxidized $[2Fe2S]^{2+}$ SoxR *in vitro* through 80 bp of well-stacked DNA.[106] DNA CT thus provides a mechanism for activation of SoxR at long range during oxidative stress.

Recent studies of the bacterial miniferritin Dps also suggest that DNA CT can be used by many different proteins in order to preserve genomic integrity. Dps is associated with the virulence of pathogenic bacteria and their ability to tolerate oxidative stress.[107] This protein can bind DNA nonspecifically and employs ferroxidase chemistry to deplete the surroundings of Fenton reagents such as Fe^{2+} and H_2O_2.[108] We demonstrated that Dps is capable of neutralizing guanine radicals through DNA CT using flash-quench techniques.[109] A $[Ru(phen)(dppz)(bpy′)]^{2+}$ (bpy′= 4-butyric acid-4′-methyl-2,2′-bipyridine) complex which intercalates into duplex DNA was tethered to one end of a 70-nt DNA substrate. Upon irradiation, this oxidant creates guanine radicals at the 5′-G of a 5′-GGG-3′ triplet site engineered into the DNA sequence. DNA-bound ferrous iron-loaded Dps, but not apo-Dps or ferric iron-loaded Dps, reduced the oxidized guanine radical from a distance through DNA CT. (Figure 5) Long-range redox chemistry can thus be employed by many different proteins with a diverse array of structural and functional properties, if these proteins can bind duplex DNA and effectively couple into the π-stacked bases.

6. DNA Charge Transport Signaling By Base Excision Repair Glycosylases coordinating a [4Fe4S] Cluster

As the evidence grew that DNA CT could be exploited for rapid and long-range redox sensing and signaling, exploring how DNA CT could be involved in other cellular processes essential for genome stability became increasingly important.[110] As discussed above, our attention turned to an emerging class of nucleic acid processing enzymes that coordinate [4Fe4S] clusters.[62] For most repair enzymes discovered to date, the biochemistry of the pathways and the implications for the etiology of disease states have already been exquisitely characterized, and many exhaustive reviews are available.[111–132] The biochemical role of the [4Fe4S] cluster in DNA repair enzymes, however, remained unclear for a long time after the cofactor was demonstrated to be present. Though the [4Fe4S] cluster is a well known and versatile metallocenter found in all domains of life that serves as a redox cofactor in many major biochemical systems,[64] it was first hypothesized that the cluster primarily has a structural role in DNA-binding repair enzymes.[62] Many of these proteins, however, do not require the cluster for stability or protein folding.[55,133] There is evidence that a stable and intact cluster is necessary for substrate recognition and turnover but not for a role in catalysis, suggesting a regulatory role for the cluster in enzymatic

function.[55,133,134] One might furthermore expect, given the possibility of Fenton chemistry with the iron-sulfur clusters near DNA, that a more redox-inert structural motif would better stabilize DNA binding.[64]

The first proteins containing [4Fe4S] clusters studied from the perspective of DNA CT were from the base excision repair (BER) pathway. Some BER substrates include, for example, apurinic/apyrimidinic sites, 7,8-dihydro-8-oxo-2′-deoxyguanosine (8-oxo-G):A mismatches, alkylated or oxidized bases, and uracil that has been incorrectly incorporated into the genome.[112] In 1989, Endonuclease III (EndoIII), an N-glycosylase and AP-lyase from *E. coli* that senses damaged pyrimidines, was the first DNA repair enzyme containing a [4Fe4S] cluster to be discovered. EndoIII coordinates the cluster in a Cys-X_4-Pro-X-Cys-X_2-Cys-X_5-Cys loop located near the C terminal domain (CTD).[53] The cluster is strongly conserved in all domains of life. The presence of the cluster was initially a surprise, but the discovery of the cluster in EndoIII was quickly followed by prediction and demonstration of a cluster in a homologous *E. coli* enzyme, MutY, a glycosylase which resolves 8-oxo-G:A lesions, and like EndoIII, is strongly conserved in prokarya, eukarya, and archaea.[135–137] The third BER enzyme, family 4 Uracil-DNA glycosylase from the thermophilic bacterium *Archeoglobus fulgidus*, (*Af*UDG), was additionally found to coordinate a [4Fe4S] cluster.[56] Thermophilic family 4 UDGs are the only known UDGs to contain a [4Fe4S] metallocenter; in most bacteria UDG does not contain a cluster but is in very high concentrations in the cell (in contrast to the BER enzymes with clusters). It is also interesting that cytosine deamination, which generates uracils within DNA, is overwhelmingly favored at the higher temperatures of thermophiles.

Structural characterization of the BER glycosylases has been instrumental in efforts to understand why a metabolically expensive and potentially reactive [4Fe4S] metallocenter would be found in enzymes that interact directly with DNA.[54,138–140] First, structures for EndoIII, MutY, and UDG from *Thermus thermophilus* (TfUDG, homologous to AfUDG) consistently show that the cluster is located remotely from the enzymatic active site, where a base is flipped out and excised; it is therefore unlikely that the cluster is directly involved in active site catalysis (Figure 6) [119]. The DNA-free and DNA-bound structures of EndoIII and MutY are moreover remarkably similar, so a large conformational change is not associated with DNA binding. Secondly, in DNA-bound crystal structures of EndoIII and MutY, the cluster is consistently located roughly 15–20 Å away from the double helix with a pathway of aromatic amino acids sandwiched between the cluster and the DNA substrate.[74,88,89] Given the pioneering work by the Gray group on protein electron transfer pathways,[141–147] the aromatic residues are highly suggestive of an electron transfer pathway from the DNA to the cluster. Hence, given these characteristics of the clusters in the repair enzymes, we were prompted to begin determining if the [4Fe4S] clusters coordinated by DNA repair proteins were redox active and could participate in DNA CT chemistry.

Initial efforts by others to study the redox chemistry of the [4Fe4S] cluster in EndoIII were met with several challenges. The cluster was purified in the $[4Fe4S]^{2+}$ oxidation state (formally two ferric and two ferrous irons), and the cluster oxidation states were difficult to access with redox mediators.[53] The $[4Fe4S]^{2+}$ degraded to the $[3Fe\text{-}4S]^{1+}$ species in the presence of ferricyanide, and the $[4Fe4S]^{1+}$ species could only be isolated by anaerobic

photoexcitation which generated powerful radical reductants *in situ* resulting in an estimated reduction potential of < −600 mV vs. NHE.[53] These initial attempts to oxidize and reduce the EndoIII cluster were, however, carried out in the absence of DNA, a polyanion that would surely affect DNA-bound redox potentials. Our approach was to adapt the DNA-modified gold electrode platform for protein electrochemistry, using EndoIII, MutY, and A*f*UDG rather than small molecules as the redox probes.[88,89] Interestingly, reversible redox activity for all three glysosylases in the presence of DNA was seen by cyclic voltammetry (CV), with positive, midpoint potentials between 60 and 100 mV vs. NHE, which is characteristic of high iron potential [4Fe4S] proteins (HiPIPs) (Figure 7).[148] Critically, there was not any observed degradation of the cluster under these conditions. Redox activity could not be observed in the absence of DNA or was greatly attenuated in the presence of an abasic site. Though abasic sites are not direct substrates of EndoIII, MutY, or UDG, the redox sensing of this DNA lesion by the BER glycosylases was an exciting discovery, and together, these data indicated that the redox activity of the [4Fe4S] cluster was facilitated and mediated by DNA (Figure 7).

The newly discovered [4Fe4S] redox activity on DNA highlighted several key features of this unrealized mode of biological electron transfer. While there is not a marked conformational change associated with DNA binding, protein binding to DNA appears to have a dramatic effect on the potential of the $[4Fe4S]^{3+/2+}$ couple. The $[4Fe4S]^{2+}$ resting state of the HiPIP glycosylases appeared to be activated toward oxidation within a potential range that is biologically accessible and does not damage the DNA bases, even within guanine repeat sequences.[149,150] On a graphite electrode, where DNA-bound and dissociated forms can be compared directly, the shift in potential was found to be ~100 mV negative on DNA binding.[151] The oxidation state of [4Fe4S] clusters is known to vary widely depending on the local environment,[148, 152] and the shift in potential with the BER glycosylases is readily explained by the change from a solvent-exposed cluster in the DNA-free state to the more negatively-charged local environment in the DNA-bound state.[89] Certainly the application of [4Fe4S] clusters in these enzymes offered an opportunity to tune the potential of the cluster to a redox-active form at cellular potentials when bound to DNA.

7. DNA CT Signaling Activity by DNA Helicases with [4Fe4S] Clusters

Concurrent to the initial characterization of the BER glycosylases, a burst of proteins involved in genome maintenance from repair, replication, recombination, and transcription were reported to coordinate a [4Fe4S] cluster.[30,31,66] Very quickly, there was ample opportunity to study the redox chemistry of many other [4Fe4S] enzymes in repair pathways other than BER. We initially focused, as introduced above, on two ATP-dependent, 5′-3′ Superfamily 2 Helicases, XPD and DinG. XPD is an essential component of the transcription factor IIH (TFIIH) machinery that unwinds DNA during nucleotide excision repair (NER) and transcription in archaea and eukarya.[131] Mutations in the XPD gene are associated with trichothiodystrophy, Cockayne syndrome, and Xeroderma pigmentosum. As with the BER glycosylases, many mutations in XPD associated with genetic diseases are known, but how some of these mutations lead to disease remained poorly understood.[75,92] Interestingly, evidence now points to an association between cluster destabilization and disease development. The second helicase we examined, DinG, is an *E. coli* SOS-inducible

protein that shares some sequence homology with XPD, most strongly in the [4Fe4S] cluster domain.[58,153] DinG is responsible for resolving R-loops (DNA:RNA duplexes) and is required for maturation of R-loops at stalled replication forks.

When *Sa*XPD from the archaea and DinG from *E. coli* were studied electrochemically on the DNA-modified gold electrode platform, both helicases were found to participate in DNA CT chemistry.[73,92] Furthermore, they shared the same DNA-bound redox potential as the BER glycosylases, approximately 80mV vs. NHE.[73,92] Consistent with the previous studies of BER [4Fe4S] enzymes, the signal was attenuated, but not shifted, in the presence of an intervening lesion (a mismatch in these studies, also not a substrate for the enzymes). Further probing of the CT activity found that in the presence of ATP, the signal for S*a*XPD and DinG quite stunningly increased in a concentration-dependent manner without any shift in the midpoint potential. Hence, it appears that helicase activity increases the electrochemical signal and coupling of the cluster to the π-stacked DNA bases, signaling electrochemically that the helicase is active. This electrical detection of redox-independent enzymatic activity by the helicases on DNA substrates is thus yet another intriguing indication of a redox role for the [4Fe4S] cluster and DNA CT in DNA biology. Indeed, two mutants of S*a*XPD, G34R and L325V (L461 in human XPD), associated with disease, were both found to be CT-deficient, but enzymatically active.[75,92] Additional studies will be instructive in how CT signaling of enzymatic activity might be utilized *in vivo*.

8. A Model for Lesion Detection Using DNA CT

With the discovery of the DNA CT redox activity of the [4Fe4S] cluster and that redox activity depends upon DNA binding, we sought to explore roles for this chemistry within the cell. One essential protein function CT deficiency could impair is the ability to detect and localize to damaged bases. Repair proteins are challenged with the enormous task of discriminating the billions of unmodified bases from the thousands of damage sites generated per day, many of which are structurally very similar to their undamaged counterparts.[110] The protein traffic on DNA in the form of transcription factors, other repair proteins, RNA polymerases, DNA polymerases, and histones (in eukaryotes) adds layers of complexity to the processes that must be coordinated in order to maintain genomic integrity. Furthermore, in *E. coli* the copy numbers of MutY and EndoIII per cell are limiting: MutY is expressed at ~30 copies/cell and EndoIII is expressed at ~500 copies/cell.[30,31] Indeed, a basic model of genome scanning that includes facilitated diffusion constants for the *E. coli* genome (4.6×10^6 base pairs) and a protein copy number of 30 under the assumption of instantaneous lesion detection and no protein traffic predicts a search time of 46 minutes to find a single lesion, far too long for an organism with an average doubling time of 20–30 min.[72] Hence other factors must facilitate efficient lesion detection.

Detection of damaged lesions through DNA CT, which is exquisitely sensitive to perturbations to the base stack (even to lesions that do not distort the helix) and an excellent reporter of base stack integrity, is one such mechanism that could enhance the DNA damage search efficiency. This mechanism may be especially relevant for proteins expressed at low copy numbers. Utilization of DNA CT in the cell for more efficient lesion detection could

explain why many DNA repair enzymes coordinate a redox-active [4Fe4S] cofactor. As such, a new model for DNA-mediated sensing and signaling *as a first step* in lesion detection was proposed based on the DNA-bound redox behavior and the shared midpoint potential of the [4Fe4S] repair enzymes (Figure 8).[30,31,72,89]

In this model, iterative signaling across the genome involves redox communication between a protein donor in the $[4Fe4S]^{2+}$ state (the resting state for HiPIP proteins, and favored in the reducing cellular environment) and a distally-bound acceptor, already in the $[4Fe4S]^{3+}$ state. We have seen that guanine radicals, presumably generated under oxidative stress, can oxidize the clusters of DNA-bound repair proteins, generating the $[4Fe4S]^{3+}$ state.[89] Upon binding to DNA, the donor is activated toward oxidation and can reduce the distally bound acceptor protein in a self-exchange electron transfer reaction if the intervening DNA is free of lesions. The acceptor, now in the $[4Fe4S]^{2+}$ state, can more easily diffuse away to another region of the genome due to the decreased binding affinity of the protein for DNA once in the reduced state. This iterative process can repeat to facilitate communication between [4Fe4S] proteins in the same repair pathway or in different repair pathways. If, however, there is a lesion between the donor and acceptor pair, redox signaling is disrupted and the lesion is sensed by the cluster proteins on either side of the lesion. The [4Fe4S] proteins bound on either side of the lesion become "trapped" on the DNA in the $[4Fe4S]^{3+}$ state, and the proteins that are "trapped" on the damaged DNA strand can then move processively on the double helix to localize to the precise location of the lesion. Proteins "trapped" on damaged strands can also recruit other protein complexes necessary for timely repair. Including a CT search component in the model of genome scanning with CT distances of only a few hundred bases predicts that a protein with a copy number as low as 10 can scan the genome for lesions in 6 minutes, which is within reason for *E. coli*.[72]

9. Cooperative, Redox Signaling Between [4Fe4S] Proteins

A key component of the proposed CT scanning model is the localization of CT-proficient, [4Fe4S] cluster proteins in the vicinity of damage, after scanning undamaged regions of the genome. A way to visualize how [4Fe4S] proteins distribute onto damaged versus undamaged DNA was developed using AFM.[72] For the AFM redistribution assay, two sets of DNA substrates, one which includes long, well-matched (WM), 3.8 kb duplex DNA and one which includes long, mismatched (MM) DNA (3.8 kb) engineered to contain a single C:A mismatch but is otherwise identical to the WM strand, are prepared. Both WM and MM DNA samples also include shorter strands (1.6 and 2.2 kbp) of undamaged DNA. EndoIII, S*a*XPD, and DinG were all studied as uniform samples and in mixtures with other [4Fe4S] repair proteins using the AFM redistribution assay. An increased density of protein was consistently found on long, MM DNA relative to the shorter, undamaged DNA substrates.[72–75] Remarkably, comparable binding density ratios of approximately 1.5 (MM/short, undamaged, see Figure 9) were observed for all CT-proficient repair proteins studied thus far, even though C:A mismatches are not native substrates for any of the enzymes studied. In stark contrast to the WT [4Fe4S] proteins, all the CT-deficient mutants visualized by AFM, EndoII Y82A, EndoIII Y75A, and SaXPD L325A, were found to have a binding density ratio of 1, showing no preference for the long, MM strand. Indeed, a direct correlation was found between the electrochemical signal of a given protein cluster on the

DNA-modified electrode, a measure of DNA CT ability, and the binding density ratio seen in the redistribution assay, a measure of the ability of the repair protein to find the mismatched strand.[74] Moreover, mixtures of wild type protein and CT-deficient mutants, for example EndoIII:Y82A and wild type EndoIII, or XPD mixed with XPD:L325V, also were found to have a binding density ratio of 1, consistent with the idea that CT-deficient mutants cannot participate in signaling to another protein.[72,75]

We have additionally used the AFM redistribution assay to monitor communication between signaling partners from *distinct* repair pathways.[73] Binding density ratios of samples containing mixtures of BER glycosylase EndoIII and R-loop repair helicase DinG were found to be comparable to binding density ratios found for samples containing only EndoIII, DinG, or XPD (Figure 9). Consistent with these findings, protein mixtures containing DinG and CT-deficient Y82A (Figure 9), did not show a preference for damaged DNA. In fact, AFM studies with signaling partners from *different* organisms, EndoIII (*E. coli*) and XPD (*S. acidocaldarius*), showed a higher density of proteins on the mismatched strands of DNA, again with a binding density ratio of 1.5, just as were found for mixtures of proteins from the same organism.[75] Furthermore, no preference for damaged DNA was seen in protein mixtures containing XPD: EndoIII Y82A, EndoII: XPD L325V, and EndoIII Y82A: XPD L325V. These findings were remarkable, and suggested to us that signaling between [4Fe4S] cluster proteins is not dependent on the type of protein (endonuclease, glycosylase, or helicase) or even on the native organism. What forms the basis for the long range signaling is the ability of these proteins to bind DNA and couple their clusters electronically to the π-stacked bases in the DNA duplex. Thus these results are fully consistent with a model of lesion detection through long-range, DNA-mediated redox signaling between [4Fe4S] repair proteins. CT-deficient mutants that cannot fully participate in DNA CT chemistry are unable to sense the lesions electrochemically, which impairs the search efficiency (redistribution onto damaged strands).

After observing robust and consistent evidence for DNA-mediated redox signaling *in vitro*, we next turned to genetics assays to probe for DNA-mediated signaling *in vivo*. The general strategy of the *in vivo* assay is to select a strain of *E. coli* that relies on the repair protein for its survival, then genetically knockout a putative signaling partner containing the [4Fe4S] cluster, and monitor how the absence of the signaling partner affects activity/survival (Figure 10). If DNA-mediated CT is used to scan the genome for lesions, then decreasing the number of signaling partners in the cell should have a measurable effect on growth. Any growth defects should also be reversible, and to pinpoint the basis for rescue, complementation plasmids are introduced into the knockout strains to express either the wild type signaling partner or mutants that are CT-deficient and enzymatically active or redox-active but enzymatically inactive.

The first *in vivo* assay we developed reports on the repair activity of MutY in the CC104 strain of *E. coli*.[72] The CC104 strain contains a cytosine rather than an adenine in the *lacZ* gene at the Glu-461 codon which is essential for metabolizing lactose (Figure 10).[154] When MutY activity is impeded, an increase in GC-to-TA transversions occurs, restoring the *lacZ* gene and growth (revertants) on minimal media where the only carbon source is lactose. When EndoIII or DinG genes (*nth* and *dinG*, respectively) are knocked out of the

CC104 strain, a significant, but not dramatic (roughly two-fold) increase in revertants is observed (Figure 10).[72] To test if the wild type phenotype could be restored, complementation plasmids were introduced expressing either Y82A, the CT-deficient but catalytically active EndoIII mutant, or D138A, which is a catalytically inactive but CT-proficient mutant of EndoIII. Consistent with our CT scanning model, the Y82A plasmid could not restore the wild type phenotype, but the D138A plasmid could restore the wild type phenotype for both EndoIII and DinG knockout strains. Thus, the ability of MutY to find lesions relies on redox signaling with EndoIII[72] and DinG[73] to find lesions, and moreover, the enzymatic functions of EndoIII and DinG do not appear to be relevant to this process.

To probe the signaling network further, another, more sensitive *in vivo* assay was developed that reports on the repair activity of DinG in the Inverted A (InvA) strain of *E. coli*.[155] In the InvA strain, the highly-transcribed rrnA operon in inverted, which increases the frequency of collisions between transcription and replication machinery and the formation of R-loops (Figure 10). DinG is required for resolving these types of lesions, and so, to test if DNA-mediated CT signaling is needed for DinG repair activity, the EndoIII gene was knocked out in the InvA strain, and growth rescue was attempted with plasmids expressing Y82A or D138A. The growth of the InvA *Δnth* mutant strain is severely compromised, but, growth can be completely rescued with the D138A plasmid, whereas the Y82A plasmid did not have a measurable effect on growth (Figure 10).[72] Like MutY, DinG also appears to rely on DNA CT chemistry to repair lesions. The ability of a catalytically inactive EndoIII enzyme (D138A) to rescue growth to wild type levels appears to be achieved simply through the increase of cellular concentration of redox-active [4Fe4S] protein to help in scanning the genome. Results from genetics assays reporting on both MutY[72,73] and DinG[73] activity thus highlight the power of DNA CT that is only now beginning to be realized in DNA and RNA biological processes. As other DNA-processing proteins containing [4Fe4S] clusters are discovered, we will be able to continue testing how DNA CT may be used in redox signaling networks.

10. Summary and Outlook

Charge transport through the π-stacked bases at the center of the DNA helix occurs over long range and in a rapid manner gated by the dynamic motion of DNA bases in solution. DNA-mediated charge transport is moreover dependent on the coupling of electron donors and acceptors to the base stack, and on the stacking interactions between the π orbitals of the nitrogenous bases. Base-pair mismatches, bulky oxidative lesions, and severe bending of the helix all attenuate DNA CT; this property is exquisitely sensitive to structural perturbations affecting π-stacking. These fundamental characteristics of DNA charge transport are utilized by DNA-binding redox active proteins both to sense oxidative damage at a distance and participate in long-range protein-protein redox signaling. Using a variety of platforms including biochemical and genetic studies, we have observed that DNA-binding enzymes containing [4Fe4S] clusters are capable of signaling one another through well-matched duplex DNA. Repair enzymes redistribute in the vicinity of oxidative lesions as a result of DNA-bound redox activity, where DNA CT appears to be harnessed by the cell as a first step in locating damaged DNA for repair.

As enzymes central to DNA-processing pathways, including eukaryotic DNA replication,[60,156] have also been discovered to contain essential [4Fe4S] cofactors, it remains now to uncover the functional role of these clusters in DNA processing. Does long-range electron transfer between DNA polymerases containing [4Fe4S] clusters play a part in coordinating the dynamic and complex process of genome duplication? What other enzymes in DNA-processing pathways contain a [4Fe4S] cluster? Continued work is necessary and important for illuminating how Nature uses the elegant and powerful chemistry of DNA charge transport in biological systems.

Acknowledgments

We are grateful to our many coworkers and collaborators for their contributions to this research. We are also especially grateful to our colleague, Harry Gray, for many insights, both respect to protein electron transfer and beyond! E.O.B. thanks the NIH for training and R.M.B.S. thanks the NSF for fellowship support. We are also grateful to the NIH (GM61077) and the Moore foundation for their financial support.

References

1. Lill R. Nature. 2009; 460:831–838. [PubMed: 19675643]
2. Lenaz G, Genova ML. Am J Physiol: Cell Physiol. 2007; 292:C1221–C1239. [PubMed: 17035300]
3. Brettel K, Leibl W. BBA. 2001; 1507:100–114. [PubMed: 11687210]
4. Gray HB, Winkler JR. BBA. 2010; 1797:1563–1572. [PubMed: 20460102]
5. Saraste M. Science. 1999; 283:1488–1493. [PubMed: 10066163]
6. Hinchliffe P, Sazanov LA. Science. 2005; 309:771–774. [PubMed: 16051796]
7. Sazanov LA, Hinchliffe P. Science. 2006; 311:1430–1436. [PubMed: 16469879]
8. Tsukihara T, Aoyama H, Yamashita E, Tomizaki T, Yamaguchi H, Shinzawa-Itoh K, Nakashima R, Yaono R, Yoshikawa S. Science. 1995; 269:1071–1074.
9. Sun F, Huo X, Zhai YJ, Wang AJ, Xu JX, Su D, Bartlam M, Rao ZH. Cell. 2005; 121:1043–1057. [PubMed: 15989954]
10. Iwata S, Lee JW, Okada K, Lee JK, Iwata M, Rasmussen B, Link TA, Ramaswamy S, Jap BK. Science. 1998; 281:64–71. [PubMed: 9651245]
11. Abrahams JP, Leslie AGW, Lutter R, Walker JE. Nature. 1994; 370:621–628. [PubMed: 8065448]
12. Xia D, Esser L, Yu L, Yu CA. Photosynth Res. 2007; 92:17–34. [PubMed: 17457691]
13. Blanco-Rodriguez AM, Busby M, Ronayne K, Towrie M, Grădinaru C, Sudhamsu J, Sýkora J, Hof M, Zális S, Di Bilio AJ, Crane BR, Gray HB, Vlček A Jr. J Am Chem Soc. 2009; 131:11788–11800. [PubMed: 19639996]
14. Warren JJ, Herrera N, Hill MG, Winkler JR, Gray HB. J Am Chem Soc. 2013; 135:11151–11158. [PubMed: 23859602]
15. Tezcan FA, Crane BR, Winkler JR, Gray HB. Proc Natl Acad Sci U S A. 2001; 98:5002–5006. [PubMed: 11296248]
16. Shih C, Museth AK, Abrahamsson M, Blanco-Rodriguez AM, Di Bilio AJ, Sudhamsu J, Crane BR, Ronayne KL, Towrie M, Vlcek A, Richards JH, Winkler JR, Gray HB. Science. 2008; 320:1760–1762. [PubMed: 18583608]
17. Winkler JR, Gray HB. J Am Chem Soc. 2014; 136:2930–2939. [PubMed: 24499470]
18. Plekan O, Feyer V, Richter R, Coreno M, Prince KC. Mol Phys. 2008; 106:1143–1153.
19. Murphy CJ, Arkin MR, Jenkins Y, Ghatalia ND, Bossmann S, Turro NJ, Barton JK. Science. 1993; 262:1025–1029. [PubMed: 7802858]
20. Stemp EDA, Arkin MR, Barton JK. J Am Chem Soc. 1995; 117:2375–2376.
21. Arkin MR, Stemp EDA, Holmlin RE, Barton JK, Hoermann A, Olson EJC, Barbara PF. Science. 1996; 273:475–480. [PubMed: 8662532]
22. Hall DB, Holmlin RE, Barton JK. Nature. 1996; 382:731–735. [PubMed: 8751447]

23. Kelley SO, Holmlin RE, Stemp EDA, Barton JK. J Am Chem Soc. 1997; 119:9861–9870.
24. Kelley SO, Jackson NM, Hill MG, Barton JK. Angew Chem, Int Ed Engl. 1999; 38:941–945.
25. Kelley SO, Barton JK. Science. 1999; 283:375–381. [PubMed: 9888851]
26. Nunez ME, Hall DB, Barton JK. Chem Biol (Oxford, U K). 1999; 6:85–97.
27. O'Neill MA, Becker H-C, Wan C, Barton JK, Zewail AH. Angew Chem Int Ed Engl. 2003; 42:5896–5900. [PubMed: 14673930]
28. Eley DD, Spivey DI. Trans Faraday Soc. 1962; 58:411–415.
29. Sontz PA, Muren NB, Barton JK. Acc Chem Res. 2012; 45:1792–1800. [PubMed: 22861008]
30. Grodick MA, Muren NB, Barton JK. Biochemistry. 2015; 54:962–973. [PubMed: 25606780]
31. Arnold AR, Grodick MA, Barton JK. Cell Chem Biol. 2016; 23:183–197. [PubMed: 26933744]
32. Berlin YA, Burin AL, Ratner MA. J Am Chem Soc. 2001; 123:260–268. [PubMed: 11456512]
33. Grozema FC, Tonzani S, Berlin YA, Schatz GC, Siebbeles LDA, Ratner MA. J Am Chem Soc. 2008; 130:5157–5166. [PubMed: 18324767]
34. Senthilkumar K, Grozema FC, Guerra CF, Bilkelhaupt FM, Lewis FD, Berlin YA, Ratner MA. J Am Chem Soc. 2005; 127:14894–149093. [PubMed: 16231945]
35. LeBard DN, Lilichenko M, Matyushov DV, Berlin YA, Ratner MA. J Phys Chem. 2003; 107:14509–14520.
36. Kanvah S, Joseph J, Schuster GB. Acc Chem Res. 2010; 43:280–287. [PubMed: 19938827]
37. Schuster GB. Acc Chem Res. 2000; 33:253–260. [PubMed: 10775318]
38. Renaud N, Berlin YA, Ratner MA. Proc Natl Acad Sci USA. 2013; 110:14867–14881. [PubMed: 23980166]
39. Barnett RN, Cleveland CL, Joy A, Landman U, Schuster GB. Science. 2001; 294:567–571. [PubMed: 11641491]
40. Giese B, Amaudrut J, Köhler A-K, Spormann M, Wessely S. Nature. 2000; 412:318–320.
41. Jorner J, Bixon M, Langenbacher T, Michel-Beyerle ME. Proc Natl Acad Sci U S A. 1998; 95:12759–12765. [PubMed: 9788986]
42. Augustyn KE, Genereux JC, Barton JK. Angew Chem Int Ed. 2007; 46:5731–5733.
43. Drummond TG, Hill MG, Barton JK. J Am Chem Soc. 2004; 126:15010–15011. [PubMed: 15547981]
44. Yoo J, Delaney S, Stemp EDA, Barton JK. J Am Chem Soc. 2003; 125:6640–6641. [PubMed: 12769567]
45. O'Neill MA, Barton JK. J Am Chem Soc. 2004; 126:11471–11483. [PubMed: 15366893]
46. Genereux JC, Barton JK. Chem Rev (Washington, DC, U S). 2010; 110:1642–1662.
47. Cohen H, Nogues C, Naaman R, Porath D. Proc Natl Acad Sci U S A. 2005; 102:11589–11593. [PubMed: 16087871]
48. Cohen H, Nogues C, Ullien D, Danube S, Naaman R, Porath D. Faraday Discuss. 2006; 131:367–376. [PubMed: 16512384]
49. Sartor V, Boone E, Schuster GB. J Phys Chem B. 2001; 105:11057–11059.
50. Boal AK, Barton JK. Bioconjugate Chem. 2005; 16:312–321.
51. Gorodetsky AA, Ebrahim A, Barton JK. J Am Chem Soc. 2008; 130:2924–2925. [PubMed: 18271589]
52. Gorodetsky AA, Dietrich LEP, Lee PE, Demple B, Newman DK, Barton JK. Proc Natl Acad Sci U S A. 2008; 105:3684–3689. [PubMed: 18316718]
53. Cunningham RP, Asahara H, Bank JF, Scholes CP, Salerno JC, Sureus K, Münck E, McCracken J, Peisach J, Emptage MH. Biochemistry. 1989; 28:4450–4455. [PubMed: 2548577]
54. Kuo CF, McRee DE, Fisher CL, O'Handley SF, Cunningham RP, Tainer JA. Science. 1992; 258:434–440. [PubMed: 1411536]
55. Porello SL, Cannon MJ, David SS. Biochemistry. 1998; 37:6465–6475. [PubMed: 9572864]
56. Hinks JA, Evans MC, DeMiguel Y, Sartori AA, Jirichy J, Pearl LH. J Biol Chem. 2002; 277:16936–16940. [PubMed: 11877410]
57. Rudolf J, Makrantoni W, Ingledew J, Stark MJR, White MF. Mol Cell. 1996; 23:801–808.

58. Ren B, Duan X, Ding H. J Biol Chem. 2009; 284:4829–4835. [PubMed: 19074432]
59. Wu J, Dunham WR, Weiss B. J Biol Chem. 1995; 270:10323–10327. [PubMed: 7730338]
60. Weiner BE, Huang H, Dattilo BM, Nilges MJ, Fanning E, Chazin WJ. J Biol Chem. 2007; 282:33444–3345. [PubMed: 17893144]
61. Netz DJA, Stith CM, Stümpfig M, Köpf G, Vogel D, Genau HM, Stodola JL, Lill R, Burgers PMJ, Pierik AJ. Nat Chem Biol. 2012; 8:125–132.
62. Meyer J. J Biol Inorg Chem. 2008; 13:157–170. [PubMed: 17992543]
63. Rees DC, Howard JB. Science. 2003; 300:929–931. [PubMed: 12738849]
64. Rouault TA. Nat Rev Mol Cell Biol. 2015; 16:45–55. [PubMed: 25425402]
65. Netz DJA, Mascharenhas J, Stehling O, Pierik AJ, Lill R. Trends Cell Biol. 2014; 24:303–312. [PubMed: 24314740]
66. Fuss JO, Tsai C, Ishida JP, Tainer JA. BBA. 2015; 1853:1253–1271. [PubMed: 25655665]
67. Kispal G, Csere P, Prohl P, Lill R. EMBO J. 1999; 18:3981–3989. [PubMed: 10406803]
68. Lill R, Muhlenhoff U. Annu Rev Cell Dev Biol. 2006; 22:457–486. [PubMed: 16824008]
69. Lill R, Muhlenhoff U. Crit Rev Biochem Mol Biol. 2007; 42:95–111. [PubMed: 17453917]
70. Gerber J, Neumann K, Prohl C, Muhlenhoff U, Lill R. Mol Cell Biol. 2004; 24:4848–4857. [PubMed: 15143178]
71. Xu B, Zhang P, Li X, Tao N. Nano Lett. 2004; 4:1105–1108.
72. Boal AK, Genereux JC, Sontz PA, Gralnick JA, Newman DK, Barton JK. Proc Natl Acad Sci U S A. 2009; 106:15237–15242. [PubMed: 19720997]
73. Grodick MA, Segal HM, Zwang TJ, Barton JK. J Am Chem Soc. 2014; 136:6470–6478. [PubMed: 24738733]
74. Romano* CA, Sontz* PA, Barton JK. Biochemistry. 2011; 50:6133–6145. [PubMed: 21651304]
75. Sontz PA, Mui TP, Fuss JO, Tainer JA, Barton JK. Proc Natl Acad Sci U S A. 2012; 109:1856–1861. [PubMed: 22308447]
76. Slinker JD, Muren NB, Gorodetsky AA, Barton JK. J Am Chem Soc. 2010; 132:2769–2774. [PubMed: 20131780]
77. Slinker JD, Muren NB, Renfrew SE, Barton JK. Nat Chem. 2011; 3:228–233. [PubMed: 21336329]
78. Pheeney CG, Arnold AR, Grodick MA, Barton JK. J Am Chem Soc. 2013; 135:11869–11878. [PubMed: 23899026]
79. Guo X, Gorodetsky AA, Hone J, Barton JK, Nuckolls C. Nature Nanotechnol. 2008; 3:163–167. [PubMed: 18654489]
80. Wang H, Muren NB, Ordinario D, Gorodetsky AA, Barton JK, Nuckolls C. Chem Sci. 2012; 3:62–65. [PubMed: 22822424]
81. Kendrick T, Giese B. Chem Commun (Cambridge, U K). 2002; 18:2016–2017.
82. Kelly SO, Barton JK. Chem Biol (Oxford, U K). 1998; 5:413–425.
83. Lewis FD, Kalgutkar RS, Wu Y, Liu X, Liu J, Hayes RT, Miller SE, Wasielewski MR. J Am Chem Soc. 2000; 122:12346–12351.
84. Lewis F, Letsinger R, Wasielewski R. Acc Chem Res. 2001; 34:159–170. [PubMed: 11263874]
85. Lewis F, Liu X, Liu J, Miller S, Hayes R, Wasielewski M. Nature. 2000; 406:51–53. [PubMed: 10894536]
86. Kelley SO, Barton JK, Jackson NM, McPherson LD, Potter AB, Spain EM, Allen MJ, Hill MG. Langmuir. 1998; 14:6781–6784.
87. Kelley SO, Boon EM, Barton JK, Jackson NM, Hill MG. Nucleic Acids Res. 1999; 27:4830–4837. [PubMed: 10572185]
88. Boon EM, Livingston AL, Chmiel NH, David SS, Barton JK. Proc Natl Acad Sci U S A. 2003; 100:12543–12547. [PubMed: 14559969]
89. Boal AK, Yavin E, Lukianova OA, O'Shea VL, David SS, Barton JK. Biochemistry. 2005; 44:8397–8407. [PubMed: 15938629]
90. Liu T, Barton JK. J Am Chem Soc. 2005; 127:10160–10161. [PubMed: 16028914]

91. Gorodetsky AA, Green O, Yavin E, Barton JK. Bioconjugate Chem. 2007; 18:1434–1441.
92. Mui TP, Fuss JO, Ishida JP, Tainer JA, Barton JK. J Am Chem Soc. 2011; 133:16378–16381. [PubMed: 21939244]
93. Pheeney CG, Barton JK. Langmuir. 2012; 28:7063–7070. [PubMed: 22512327]
94. Muren NB, Barton JK. J Am Chem Soc. 2013; 135:16632–16640. [PubMed: 24164112]
95. Boon EM, Ceres DM, Drummond TG, Hill MG, Barton JK. Nat Biotechnol. 2000; 18:1096–1100. [PubMed: 11017050]
96. Nunez ME, Holmquist GP, Barton JK. Biochemistry. 2001; 40:12465–12471. [PubMed: 11601969]
97. Merino EJ, Barton JK. Biochemistry. 2008; 47:1511–1517. [PubMed: 18189417]
98. Kornberg RD, Lorch Y. Cell. 1999; 98:285–294. [PubMed: 10458604]
99. Luger K, Mader A, Richmond R, Sargent D, Richmond TJ. Nature. 1997; 389:251–260. [PubMed: 9305837]
100. Nunez ME, Noyes KT, Barton JK. Chem Biol (Oxford, U K). 2002; 9:403–415.
101. Kim Y, Geiger JH, Hahn SH, Sigler PB. Nature. 1993; 365:512–520. [PubMed: 8413604]
102. Demple B. Gene. 1996; 179:53–57. [PubMed: 8955629]
103. Demple B, Ding H, Jorgensen M. Methods Enzymol. 2002; 348:355–364. [PubMed: 11885291]
104. Hidalgo E, Demple B. J Biol Chem. 1996; 271:7269–7272. [PubMed: 8631739]
105. Hidalgo E, Demple B. EMBO J. 1994; 13:138–146. [PubMed: 8306957]
106. Lee PE, Demple B, Barton JK. Proc Natl Acad Sci U S A. 2009; 106:13164–13168. [PubMed: 19651620]
107. Sund CJ, Rocha ER, Tzinabos AO, Wells WG, Gee JM, Reott MA, O'Rourke DP, Smith C. Mol Microbiol. 2008; 67:129–142. [PubMed: 18047569]
108. Zhao G, Ceci P, Ilari A, Giangiacomo L, Laue T, Chiancone E, Chasteen ND. J Biol Chem. 2002; 277:27689–27696. [PubMed: 12016214]
109. Arnold AR, Barton JK. J Am Chem Soc. 2013; 135:15726–15729. [PubMed: 24117127]
110. Rajski SR, Jackson BA, Barton JK. Mutat Res, Fundam Mol Mech Mutagen. 2000; 447:49–72.
111. Demple B, Harrison L. Annu Rev Biochem. 1994; 63:915–948. [PubMed: 7979257]
112. David SS, Wiliams SD. Chem Rev (Washington, DC, U S). 1998; 98:1221–1261.
113. Lindahl T, Wood RD. Science. 1999; 286:1897–1905. [PubMed: 10583946]
114. Zhou BBS, Elledge SJ. Nature. 2000; 408:433–439. [PubMed: 11100718]
115. Hoeijmakers JHJ. Nature. 2001; 411:366–374. [PubMed: 11357144]
116. Sancar A, Lindsey-Boltz LA, Unsal-Kacmaz K, Linn S. Annu Rev Biochem. 2004; 73:39–85. [PubMed: 15189136]
117. Huffman JL, Sundheim O, Tainer JA. Mutat Res-Fundam Mol Mech Mutagen. 2005; 577:55–76.
118. Kelman Z, White MF. Curr Opin Microbiol. 2005; 8:669–676. [PubMed: 16242991]
119. Lukianova OA, David SS. Curr Opin Chem Biol. 2005; 9:145–151. [PubMed: 15811798]
120. Burgers PMJ. J Biol Chem. 2009; 284:4041–4045. [PubMed: 18835809]
121. Jackson SP, Bartek J. Nature. 2009; 461:1071–1078. [PubMed: 19847258]
122. Hiom K. DNA Repair. 2010; 9:250–256. [PubMed: 20122882]
123. Yeeles JTP, Dillingham MS. DNA Repair. 2010; 9:276–285. [PubMed: 20116346]
124. Egly JM, Coin F. DNA Repair. 2011; 10:714–721. [PubMed: 21592869]
125. Kim N, Jinks-Robertson S. Nat Rev Genet. 2012; 13:204–214. [PubMed: 22330764]
126. Brosh RM. Nat Rev Cancer. 2013; 13:542–558. [PubMed: 23842644]
127. Hamperl S, Cimprich KA. DNA Repair. 2014; 19:84–94. [PubMed: 24746923]
128. Helleday T, Eshtad S, Nik-Zainal S. Nat Rev Genet. 2014; 15:585–598. [PubMed: 24981601]
129. Tsutakawa SE, Lafrance-Vanasse J, Tainer JA. DNA Repair. 2014; 19:95–107. [PubMed: 24754999]
130. Gaillard H, Garcia-Muse T, Aguilera A. Nat Rev Cancer. 2015; 15:276–289. [PubMed: 25907220]
131. Spivak G. DNA Repair. 2015; 36:13–18. [PubMed: 26388429]

132. Rayner E, van Gool IC, Palles C, Kearsey SE, Bosse T, Tomlinson I, Church DN. Nat Rev Cancer. 2016; 16:71–81. [PubMed: 26822575]
133. Rogers PA, Eide L, Klungland A, Ding H. DNA Repair. 2003; 2:809–817. [PubMed: 12826281]
134. Engstrom LM, Partington OA, David SS. Biochemistry. 2012; 51:5187–5197. [PubMed: 22646210]
135. Michaels ML, Pham L, Nghiem Y, Cruz C, Miller JH. Nucleic Acids Res. 1990; 18:3841–3845. [PubMed: 2197596]
136. Tsai-Wu JJ, Liu HF, Lu AL. Proc Natl Acad Sci U S A. 1992; 89:8779–8783. [PubMed: 1382298]
137. Porello SL, Williams SD, Kuhn H, Michaels ML, David SS. J Am Chem Soc. 1996; 118:10684–10692.
138. Thayer MM, Ahern H, Xing D, Cunningham RP, Tainer JA. EMBO J. 1995; 14:4108–4120. [PubMed: 7664751]
139. Fromme JC, Verdine GL. EMBO J. 2003; 22:3461–3471. [PubMed: 12840008]
140. Hoseki J, Okamoto A, Masui R, Shibata T, Inoue Y, Yokoyama S, Kuramitsu S. J Mol Biol. 2003; 333:515–526. [PubMed: 14556741]
141. Gray HB, Winkler JR. Annu Rev Biochem. 1996; 65:537–561. [PubMed: 8811189]
142. Gray HB, Winkler JR. Q Rev Biophys. 2003; 36:341–372. [PubMed: 15029828]
143. Dempsey JL, Winkler JR, Gray HB. Chem Rev (Washington, DC, U S). 2010; 110:7024–7039.
144. Gray HB, Winkler JR. Biochim Biophys Acta, Bioenerg. 2010; 1797:1563–1572.
145. Warren JJ, Ener ME, Vlcek A, Winkler JR, Gray HB. Coord Chem Rev. 2012; 256:2478–2487. [PubMed: 23420049]
146. Warren JJ, Winkler JR, Gray HB. FEBS Lett. 2012; 586:596–602. [PubMed: 22210190]
147. Winkler JR, Gray HB. Chem Rev (Washington, DC, U S). 2014; 114:3369–3380.
148. Cowan JA, Lui SM. Adv Inorg Chem. 1998; 45:313–350.
149. Crespo-Hernández CE, Close DM, Gorb L, Leszczynski J. J Phys Chem B. 2007; 111:5386–5395. [PubMed: 17447808]
150. Paukku Y, Hill G. J Phys Chem A. 2011; 115:4804–4810. [PubMed: 21500846]
151. Gorodetsky AA, Boal AK, Barton JK. J Am Chem Soc. 2006; 128:12082–12083. [PubMed: 16967954]
152. Liu J, Chakraborty S, Hosseinzadeh P, Yu Y, Tian S, Petrik I, Bhagi A, Lu Y. Chem Rev (Washington, DC, U S). 2014; 114:4366–4469.
153. Voloshin ON, Vanevski F, Khil PP, Camerini-Otero RD. J Biol Chem. 2003; 278:28284–28293. [PubMed: 12748189]
154. Cupples CG, Miller JH. Proc Natl Acad Sci U S A. 1989; 86:5345–5349. [PubMed: 2501784]
155. Boubakri H, de Septenville AL, Viguera E, Michel B. EMBO J. 2010; 2003:145–157.
156. Klinge S, Hirst J, Maman JD, Krude T, Pellegrini L. Nat Struct Mol Biol. 2007; 14:875–877. [PubMed: 17704817]

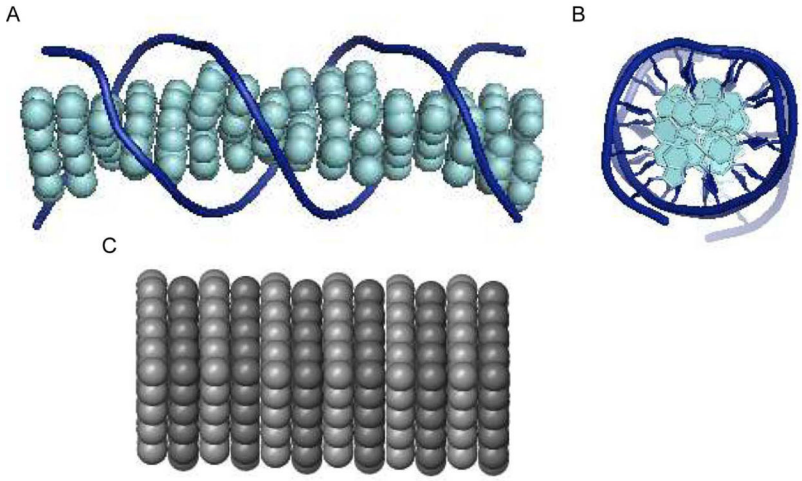

Figure 1.

The structure of DNA shows chemical similarities to graphene sheets. A) Schematic of the DNA helix. The aromatic bases at the center of the DNA helix are oriented so that the π orbitals of adjacent bases overlap with one another in the duplex DNA structure. B) Looking down the helix axis showing aromatic base pairs (light blue) stacked in 3.4Å layers at the center of DNA. C) Structure of graphite.

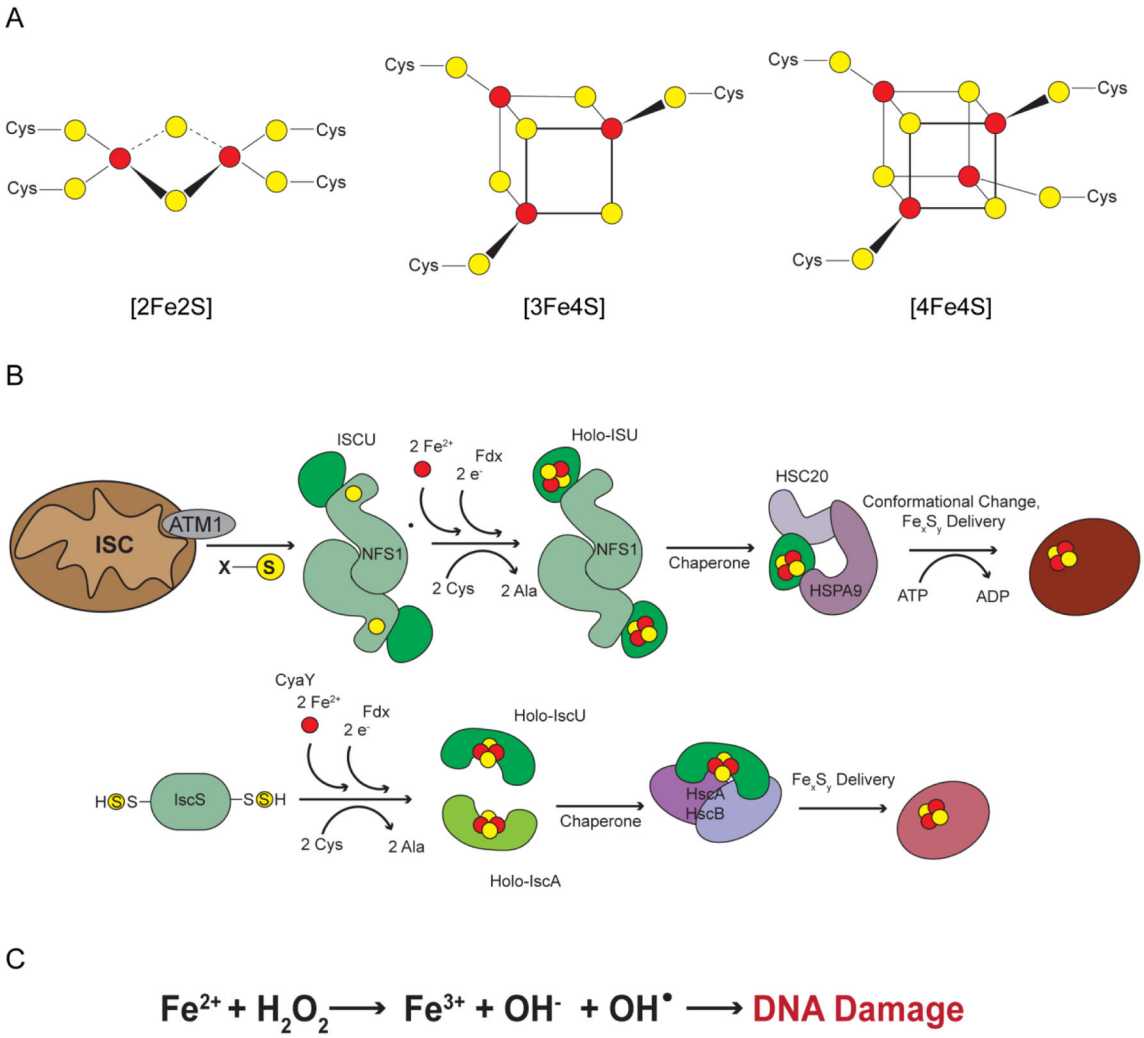

Figure 2.

Iron-sulfur clusters in biology. A) Structures of common iron-sulfur cofactors, the rhomboid [2Fe2S] cluster, the [3Fe4S] cluster, and the cubane [4Fe4S] cluster. B) Eukaryotic (above) and bacterial (below) iron-sulfur cofactor assembly and incorporation into proteins. C). Fenton chemistry.

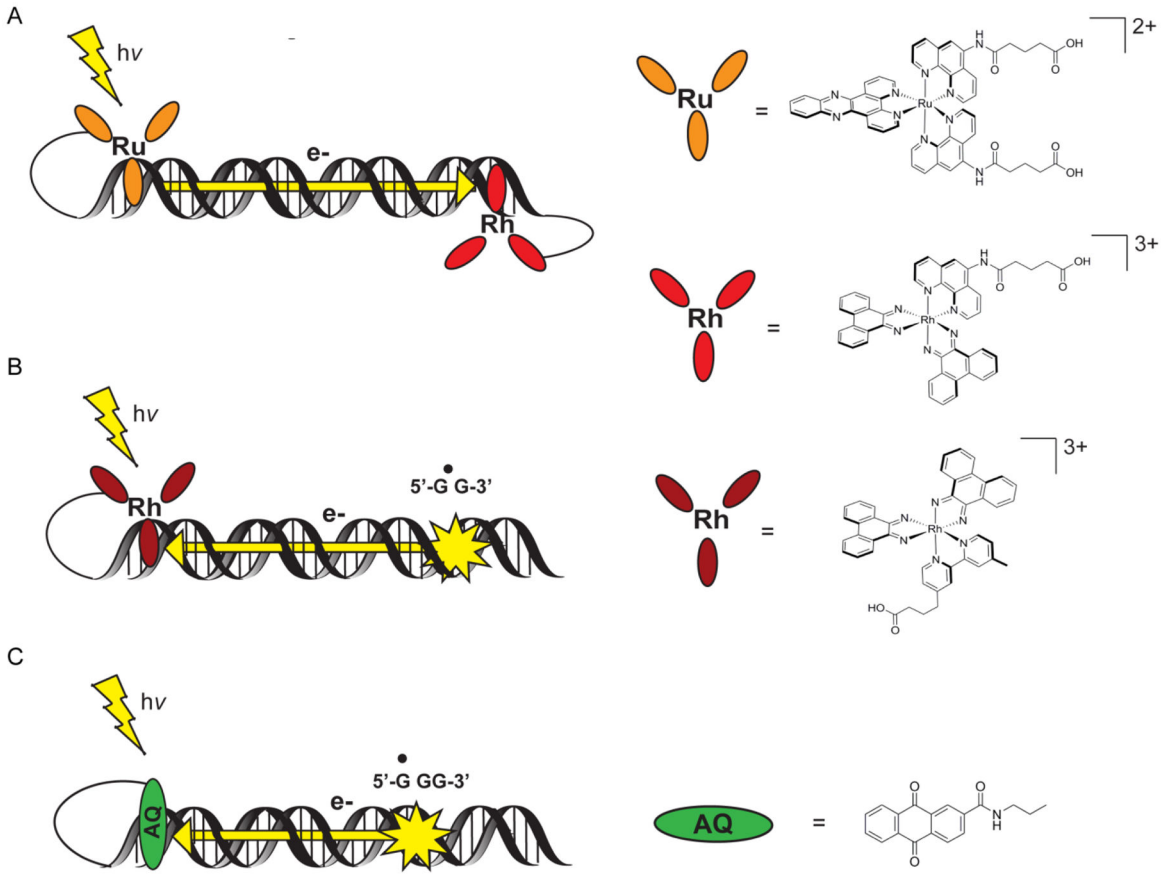

Figure 3.

Platforms to study DNA CT in the excited state. A) A covalently tethered DNA-assembly to probe long range emission quenching through DNA CT B) An assembly to monitor DNA-mediated oxidation of low-potential guanine bases by a tethered rhodium photooxidant[26] C) An assembly to monitor long range oxidative damage with a DNA-capped anthraquinone.[37,39]

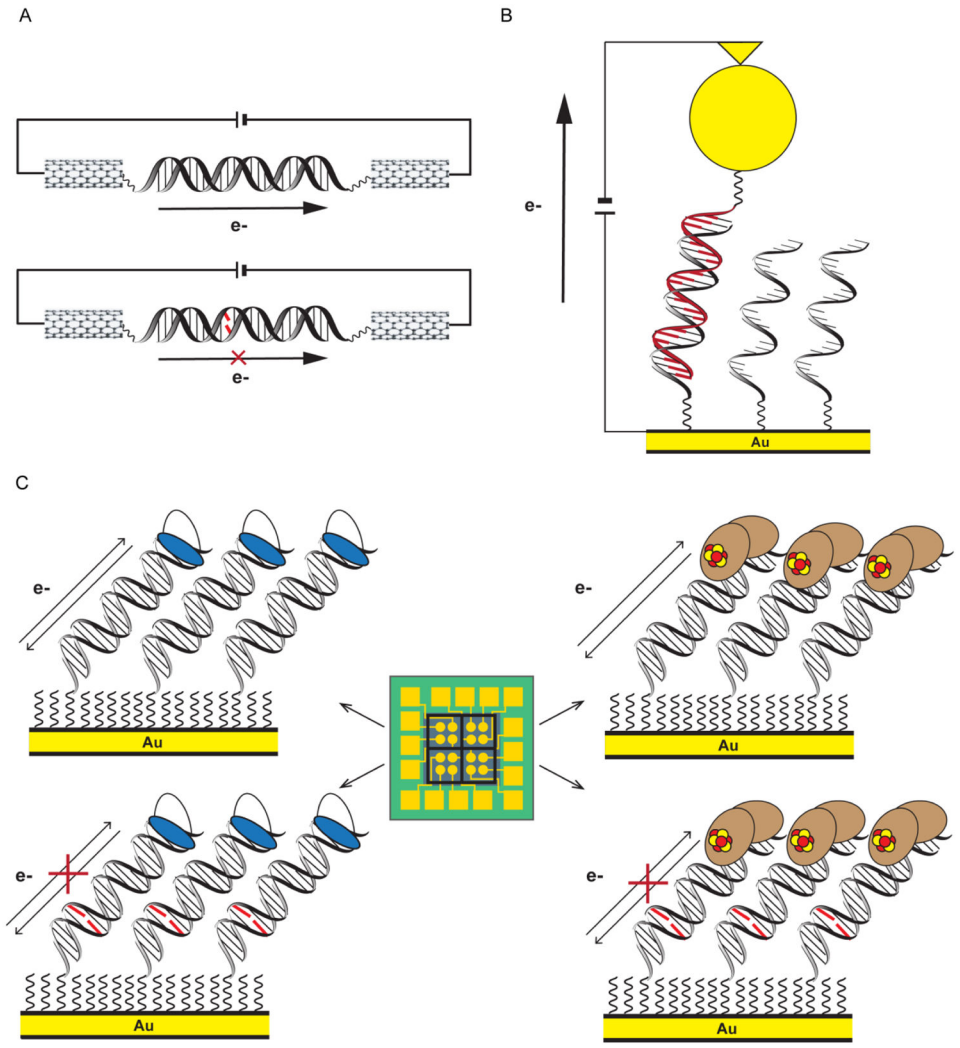

Figure 4.

Platforms to study DNA CT in the ground state. A) Single-molecule carbon nanotube device[79,80] measuring the source-drain current I_{SD} at a constant applied voltage. Significant current flow is apparent with the well matched duplex (top) but not with an an intervening mismatch (below) B) Electrochemical atomic force microscopy is used to measure current passage through an oligonucleotide duplex attached to an Au surface at one end and a Au nanoparticle at the other end.[47,48] C) Multiplexed, DNA-modified Au electrodes facilitate robust, reproducible electrochemical scans of DNA monolayers on a Au surface.[76–78] Long-range (top) and mismatch-sensitive (bottom) DNA CT to redox probes (left) or protein (right) are observed.

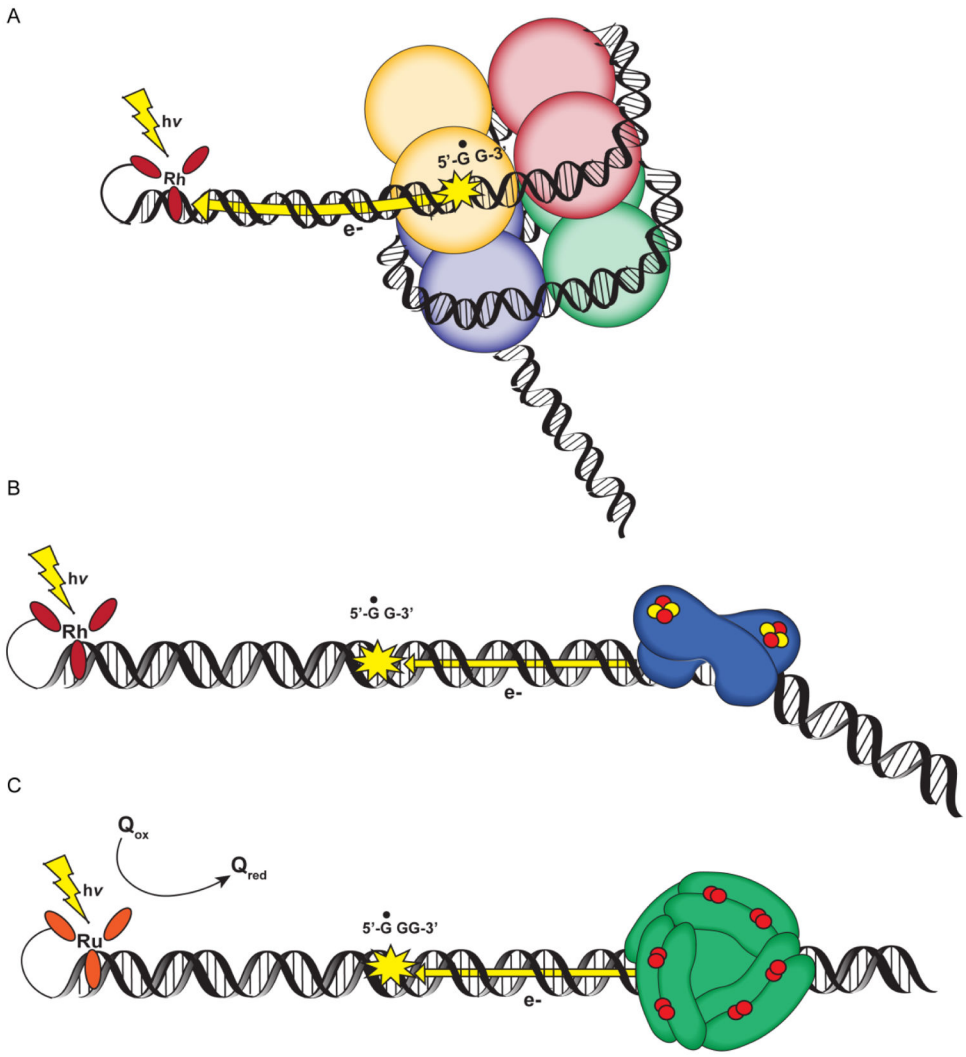

Figure 5.

DNA CT occurs in various biological assemblies. A) Long range photooxidation through a nucleosome core particle. [96] B) Long range activation of SoxR in response to oxidative stress.[106] C) Long range protection of oxidative DNA damage by Dps[109]

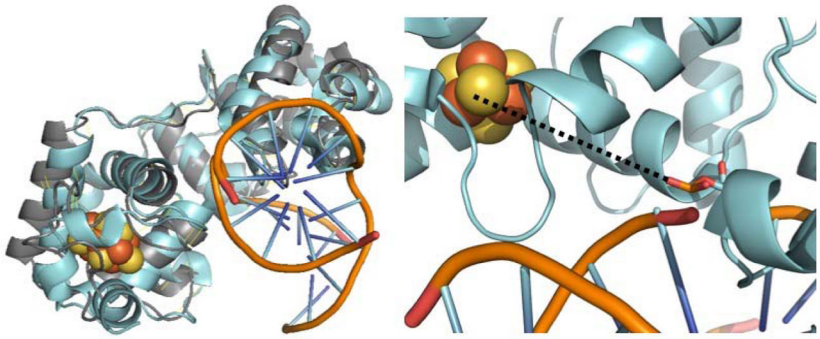

Figure 6.

Structures of Endonuclease III (EndoIII). [138,139] The overlay of the free EndoIII structure (*E. coli*, gray, PDB ID: 2ABK) and the DNA-bound structure (*T. thermophilus*, light teal, PDB ID: 1ORN) shows little change in conformation upon binding to substrate (left). In both forms, the [4Fe4S] cluster (orange and yellow spheres) is located remotely (15.2 Å) from the active site, (dotted line, right, PDB ID: 1ORP), though the cluster is in close proximity to DNA (17.1 Å). The above images were generated in PyMOL.

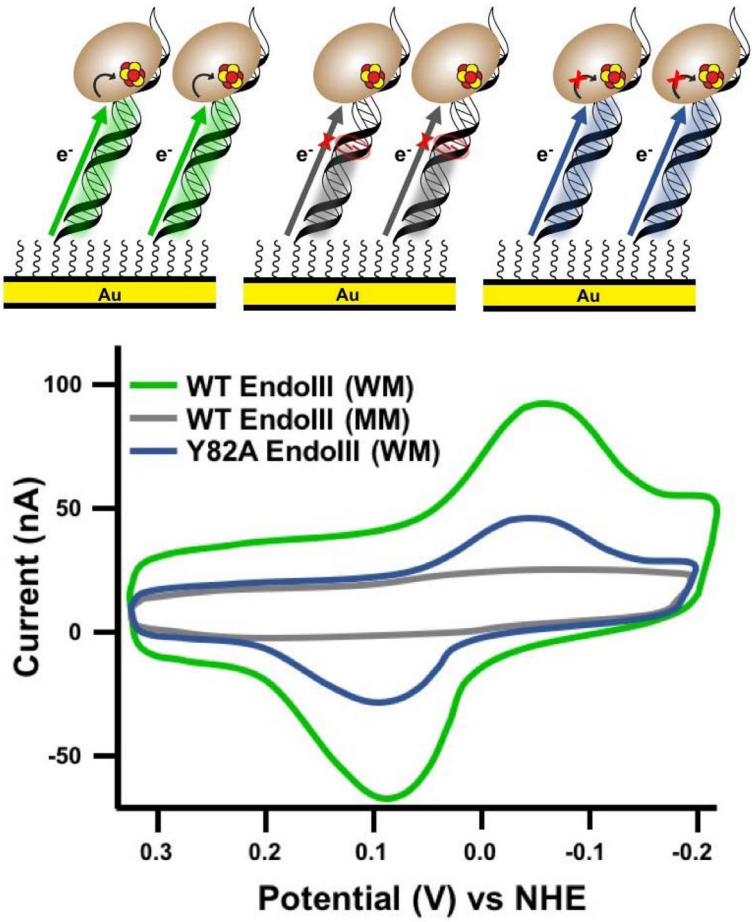

Figure 7.

DNA CT to EndoIII Electrochemically with assemblies (above) and CV's (below). For WT EndoIII (green) a reversible CV is found, that is attenuated with an intervening mismatch (grey). For the CT-deficient Y82A mutant (blue) the CV signal is also attenuated.

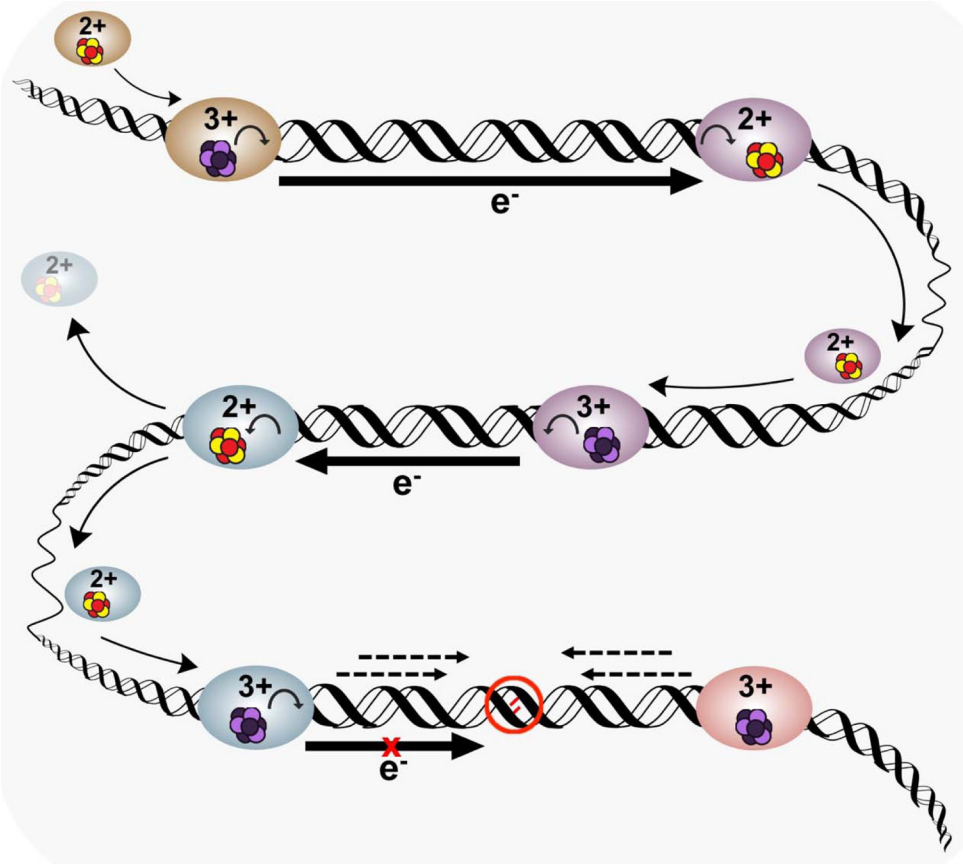

Figure 8.

A Model of DNA-mediated Redox Signaling Between [4Fe4S] DNA Processing Enzymes for Enhanced Lesion Detection.[30,31] Freely-diffusing (top left, tan oval) [4Fe4S] protein in 2+ state (red and yellow cluster) is activated toward oxidation upon binding to DNA (3+ state, light and dark purple cluster), and can reduce a distally-bound protein (mauve oval) to the 2+ state. In the 2+ state, diffusion to another region of the genome and repeated CT scanning to search for lesions (middle strand, mauve and blue ovals) can occur. If there is an intervening lesion between two signaling partners (bottom strand, blue and rose ovals), redox communication is interrupted (black arrow with red X), resulting in both proteins trapped on DNA in the 3+ state which allows for procession toward the lesion (dotted arrows) and subsequent repair of the damage.

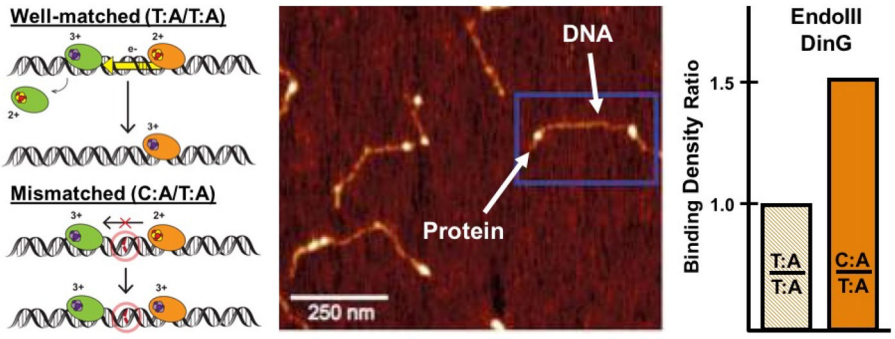

Figure 9.

Visualization of protein localization on mismatched DNA by AFM.[72–75] In the AFM redistribution assay (left), [4Fe4S] protein or protein mixtures are incubated with DNA substrates which contain either long, WM or MM strands (3.8 kbp), and short, WM DNA stands (1.6 and 2.2 kbp) and imaged (middle). The proteins bound to long strands of DNA are counted, normalized, and expressed as a binding density ratio (right). Consistently, CT-proficiency determines if redistribution the mismatched substrate occurs.

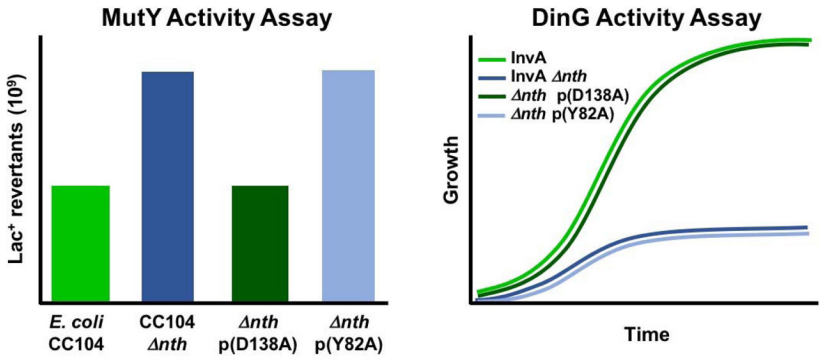

Figure 10.

Genetic Assays for Detection of DNA CT Signaling Among *E. co*li [4Fe4S] Repair Proteins.[72,73] In the MutY Activity assay (left), impaired MutY activity in the CC104 strain leads to an increase in GC to TA transversions at the *lacZ* gene and to an increase in revertants on lactose-only media. In the DinG activity assay (right), impaired activity of DinG in the InvA strainleads to a dramatic growth defect. Knocking out EndoIII (*Δnth*) impaired both MutY and DinG activity (dark blue bar, left, and dark blue curve, right). Rescue in both assays could be achieved by addition of CT-proficient, but enzymatically-inactive protein (green bar, left, and green curve, right), but not CT-deficient, though enzymatically active Y82A (light blue bar, left, and light blue curve, right).